

# Next-to-leading order QCD and electroweak corrections to Higgs-strahlung processes at the LHC

Pazilet Obul,<sup>1,2,\*</sup> Sayipjamal Dulat,<sup>1,2,†</sup> Tie-Jiun  
Hou,<sup>1,2</sup> Ablikim Tursun,<sup>1,2</sup> and Nijat Yalkun<sup>1,2</sup>

<sup>1</sup> *School of Physics Science and Technology,  
Xinjiang University, Urumqi, Xinjiang 830046 China*  
<sup>2</sup> *Center for Theoretical Physics, Xinjiang University,  
Urumqi, Xinjiang 830046 China*

## Abstract

In this paper we calculate the total and fiducial cross sections as well as differential distributions for the Higgs-strahlung or VH process  $pp \rightarrow VH \rightarrow l\nu_l/l^-l^+ + H$ , ( $V = W$  or  $Z$ ,  $l=e,\mu$ ) including QCD and electro-weak corrections up to next-to-leading order before and after reweighting photon PDFs of NNPDF2.3qed, NNPDF3.0qed, MRST2004qed, CT14QEDinc, and LUXqed at the LHC with 13 TeV and Higgs boson mass  $M_H = 125$  GeV. The predictions from the various photon PDFs before and after reweighting against each other are in good agreement. The photon PDF uncertainties of the photon-induced cross sections decrease significantly with the reweighting PDFs.

PACS numbers: 14.80.Bn,13.40.Ks,12.38.-t,05.10.Ln

Keywords: Higgs-boson; QCD correction; electro-weak correction, Reweighting-PDFs

---

\*Electronic address: pazilet.obul@hotmail.com

†Electronic address: sdulat@hotmail.com

## **Contents**

<b>I. Introduction</b>	<b>3</b>
<b>II. Results</b>	<b>4</b>
A. Feynman Diagrams	4
B. Input Parameters and Cuts	5
C. Total Cross Sections	7
D. Fiducial Cross Section	10
E. Fiducial Differential Cross Section	11
<b>III. Conclusions</b>	<b>14</b>
<b>IV. Acknowledgments</b>	<b>14</b>
<b>References</b>	<b>14</b>

## I. INTRODUCTION

The Standard Model (SM) predicts the Higgs boson, that is, the remnant of the electroweak (EW) symmetry-breaking mechanism that generates the gauge boson and fermion masses [1]. One of the most important Higgs boson production mechanisms at hadron colliders is the Higgs-strahlung process, i.e. the associated production of Higgs bosons and weak gauge bosons,

$$pp \rightarrow WH + X \rightarrow H \nu_l l + X \quad \text{and} \quad pp \rightarrow ZH + X \rightarrow H l^+ l^- + X \quad (1)$$

In order to determine the Higgs boson properties with high precision at the LHC, it is necessary to calculate the higher order quantum chromodynamics (QCD) and EW corrections. One particular EW correction of interest is that due to photons coming from the proton in the initial state. It is thus necessary to use photon parton distribution functions (PDFs) both for consistency when EW corrections are included, and because photon-induced processes can become important at high energies. So far, a number of PDF groups, namely, the MRST, NNPDF and CTEQ collaborations, have introduced photon PDFs along with PDF evolution at leading order (LO) in QED and next-to-leading order (NLO) or next-to-next-to-leading order (NNLO) in QCD. Reference [2] calculated NLO QCD corrections to the  $pp \rightarrow W^\pm H + X$  (sum of  $W^+H$  and  $W^-H$ ) and  $pp \rightarrow ZH + X$  total cross sections at the LHC at 16 TeV and 40 TeV, and discussed in detail the total cross section dependence on the choice of factorization scale and for three different sets of PDFs (MT, KMRS and DFLM) within the DIS scheme and  $\overline{MS}$  scheme for  $m_H = 100$  GeV. References [3, 6] presented the impact of the EW corrections on the cross section predictions for the processes  $pp/p\bar{p} \rightarrow W^\pm H + X$  and  $pp/p\bar{p} \rightarrow ZH + X$  at the Tevatron ( $\sqrt{s} = 1.96$  TeV) and LHC ( $\sqrt{s} = 14$  TeV) for the three different input parameter schemes ( $G_\mu$ ,  $\alpha(M_Z)$ , and  $\alpha(0)$ -schemes), and studied the theoretical uncertainties induced by factorization and renormalization scale dependence and by the PDFs by using the CTEQ6L1 and CTEQ6M [4] PDFs, respectively. The EW corrections in the  $G_\mu$  and  $\alpha(M_Z)$ -schemes are significant and reduce the cross section by 5-9% and by 10-15%, respectively. The EW corrections in the  $\alpha(0)$ -scheme are rather small. References [5, 6] discussed the NNLO QCD, i.e. the  $O(\alpha_s^2)$ , corrections to the  $pp/p\bar{p} \rightarrow W^\pm H$  and  $pp/p\bar{p} \rightarrow ZH$  production cross sections at the Tevatron at 1.96 TeV and LHC at 14 TeV for Higgs boson masses  $M_H \lesssim 200 - 300$  GeV using the MRST [7] PDFs. For  $M_H = 120$  GeV, the renormalization and factorization scale uncertainty at the LHC at 14 TeV drops from 10% at LO to 5% at NLO, and to 2% at NNLO. At the Tevatron and for the same Higgs boson mass, the scale uncertainty drops from 20% at LO to 7% at NLO, and to 3% at NNLO. A. Denner et al [8] have discussed the impact of EW radiative corrections to the Higgs-strahlung processes at the Tevatron (1.96 TeV) and LHC (7 TeV and 14 TeV) within the  $G_\mu$ -scheme for  $M_H = 120$  GeV using the HAWK Monte Carlo program. The LHC Higgs Cross Section Working Group [9] provided an update of the total and fiducial cross-section, together with theoretical uncertainties from renormalization and factorization scales, of the process  $pp \rightarrow W^\pm/Z + H \rightarrow l\nu_l/l^+l^- + H$  including NNLO QCD and NLO EW corrections

for different proton-proton collision energies ( $\sqrt{s} = 7\text{TeV}, 8\text{TeV}, 13\text{TeV}, 14\text{TeV}$ ) for a Higgs boson mass  $M_H = 125\text{GeV}$ . Reference [13] studied the impact of the CMS measurements of W boson pair production at the LHC at 8 TeV on the NNPDF2.3qed, NNPDF3.0qed [14], CT14QEDinc [15], and LUXqed [16] photon PDFs, and found that the data strongly suggest that the NNPDF photon error band should be significantly reduced. Therefore, it is necessary to re-examine the physics effects induced by photon-initiated process. In this paper, by using various PDFs, we update the predictions for the processes  $pp \rightarrow W^\pm/Z + H \rightarrow l\nu_l/l^+l^- + H$  at the LHC at 13 TeV and Higgs boson mass  $M_H = 125\text{ GeV}$ , including the NLO QCD and EW corrections using the most recent PDFs.

The paper is organized as follows. In Section II, first we give the Feynman diagrams for the Higgs-strahlung processes  $pp \rightarrow W^\pm/Z + H \rightarrow l\nu_l/l^+l^- + H$  at LO and NLO. Then we provide our numerical results for these processes at the LHC with center-of-mass energy 13 TeV using the Monte Carlo program HAWK [17] by adopting the NNPDF2.3qed, NNPDF3.0qed, MRST2004qed, CT14QEDinc, and NNLO LUXqed PDFs, as well as their reweighting photon PDFs. We obtain reweighting photon PDFs by using the reweighting method [18–21] and the LHC CMS 8 TeV data [22] as in Ref. [13]. Our conclusion is given in Section III.

## II. RESULTS

### A. Feynman Diagrams

The LO Feynman diagrams for Higgs boson production in association with weak gauge bosons  $V = W^\pm, Z$ , at the proton-antiproton collider Tevatron and proton-proton collider LHC, are shown in Fig. 1. The corresponding partonic processes are  $q_{i,u} \bar{q}_{j,d} \rightarrow HW^+ \rightarrow$

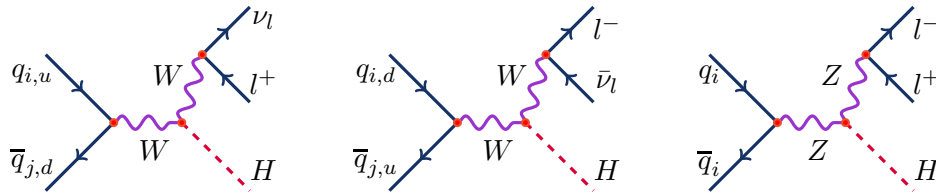
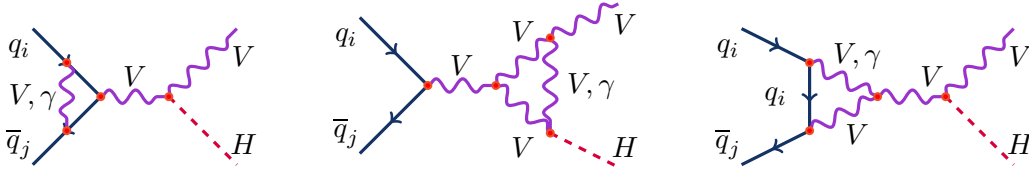


FIG. 1: Feynman diagram for Higgs-strahlung processes at LO. The straight, wavy, and dashed lines denote fermions, weak gauge bosons, and Higgs boson, respectively.

$Hl^+\nu_l$  and  $q_{i,d} \bar{q}_{j,u} \rightarrow HW^- \rightarrow Hl^-\bar{\nu}_l$ , where  $q_{i,u}$  and  $q_{i,d}$  denote up- and down-type quarks of the  $i$ th generation, as well as  $q_i \bar{q}_i \rightarrow HZ \rightarrow Hl^+l^-$ , where  $q_i$  denotes any light quark of the  $i$ th generation.

At NLO the corrections to the Higgs-strahlung process includes QCD corrections (virtual corrections with gluon exchange in the  $q\bar{q}$  vertex, gluon-induced processes, and the emission of an additional gluon) and complete EW corrections (incoming photon corrections, virtual

Vertex diagrams:



Box diagrams:

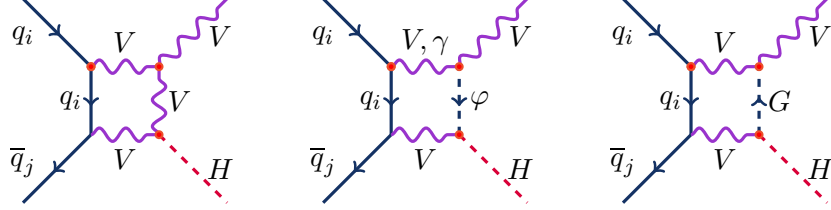


FIG. 2: Feynman diagrams corresponding to the EW virtual corrections to the LO processes.

and real EW corrections including the outgoing photon corrections). The representative Feynman diagrams for the NLO QCD and EW corrections are shown in Figs. 2, 3 and 4. The EW virtual corrections can be classified into vertex and box corrections.

In this section, we present numerical results for total and differential cross sections for associated  $W^\pm H$  ( $W^+ \rightarrow l^+ \nu_l$  and  $W^- \rightarrow l^- \bar{\nu}_l$ , where  $l = e, \mu$ ) and  $ZH$  ( $Z \rightarrow l^+ l^-$ ) production with NNPDF2.3qed, NNPDF3.0qed, MRS2004qed, CT14QEDinc, and LUXqed photon PDFs at the LHC at 13 TeV including the NLO QCD and EW corrections.

## B. Input Parameters and Cuts

In our numerical analysis of the VH processes ( $V = W^\pm, Z$ ) we use the same VH input parameters and cuts as in Ref. [9],

$$\begin{aligned}
 G_F &= 1.166378 \times 10^{-5} \text{GeV}^{-2}, & \alpha_s(M_Z) &= 0.11801, \\
 \Gamma_W &= 2.08430 \text{ GeV}, & \Gamma_Z &= 2.49427 \text{ GeV}, \\
 M_H &= 125 \text{ GeV}, & M_W &= 80.35797 \text{ GeV}, & M_Z &= 91.15348 \text{ GeV}, \\
 m_e &= 0.510998910 \text{ MeV}, & m_\mu &= 0.105658 \text{ GeV}, & m_t &= 172.5 \text{ GeV}
 \end{aligned}$$

The electromagnetic coupling is fixed in the  $G_F$ -scheme,

$$\alpha_{G_F} = \frac{\sqrt{2} G_F M_W^2}{\pi} \sin^2 \theta_W \quad (2)$$

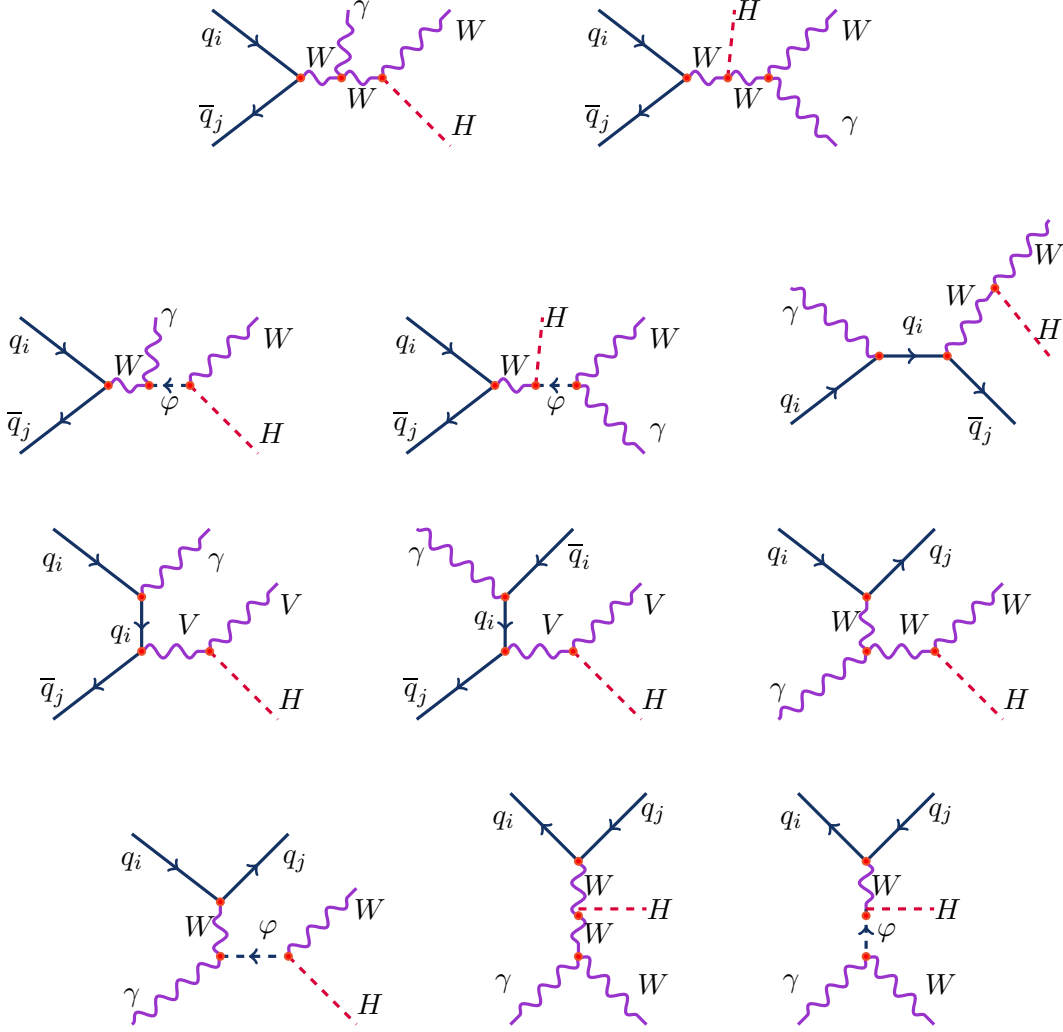


FIG. 3: Feynman diagrams corresponding to the EW real corrections to the LO processes.

and the weak mixing angle is defined in the on-shell scheme,

$$\sin^2 \theta_W = 1 - M_W^2/M_Z^2 \quad (3)$$

Both the factorization and the renormalization scales are set to the value of the invariant mass of the VH system,

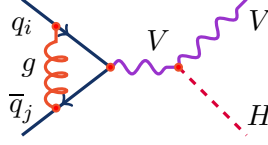
$$\mu = \mu_R = \mu_F = M_{VH}, \quad M_{VH}^2 \equiv (p_V + p_H)^2. \quad (4)$$

We also provide results for the total cross section and differential cross section in the same kinematic region as in Ref. [9],

$$p_{T_l} > 15 \text{ GeV}, \quad |y_l| < 2.5, \quad (5)$$

where  $p_{T_l}$  is the transverse momentum of the lepton and  $y_l$  is its rapidity. For  $Z(\rightarrow l^+l^-)H$

(a) Virtual diagrams:



(b) Real diagrams:

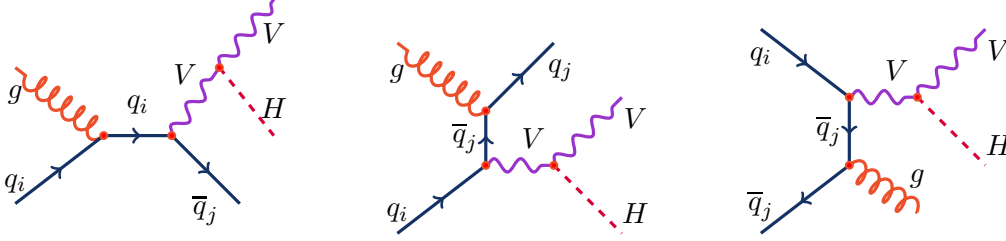


FIG. 4: Feynman diagrams corresponding to the NLO QCD corrections to the LO processes.

production the invariant mass of the two leptons is in the range

$$75\text{GeV} < M_{ll} < 105\text{GeV}. \quad (6)$$

### C. Total Cross Sections

First we study the effect of the NLO corrections on the LO cross sections without any cuts on the final-state charged leptons using the SM input parameters given in Section II B. The total NLO VH cross sections  $\sigma_{NLO}^{VH}$  and relative corrections  $\delta_{QCD/EW}$  are calculated according to

$$\sigma_{NLO}^{VH} = \sigma_{LO}^{VH}(1 + \delta_{EW} + \delta_{QCD}) + \sigma_{\gamma}, \quad (7)$$

and

$$\delta_{QCD/EW} = \frac{\sigma_{QCD/EW}}{\sigma_{LO}^{VH}} \times 100\%. \quad (8)$$

For the LO calculations, strictly speaking, one should use LO PDFs, but for convenience, we used NLO PDFs. In Tables I, II, and III we list the LO and NLO total cross sections ( $\sigma_{LO}$ ,  $\sigma_{NLO}$ ) including NLO QCD and EW corrections ( $\delta_{QCD}$ ,  $\delta_{EW}$ ), and photon-induced cross sections ( $\sigma_{\gamma}$ ,  $\sigma_{\gamma PR}$ ) with PDF uncertainties for the Higgs-strahlung processes  $pp \rightarrow W^{\pm}/Z + H \rightarrow l\nu_l/l^+l^- + H$  with NNPDF2.3qed, NNPDF3.0qed, MRS2004qed, CT14QEDinc, and LUXqed photon PDFs and Higgs-boson mass  $M_H=125$  GeV at the LHC at  $\sqrt{s}=13$  TeV. The photon-induced cross section is only significant for WH production. Note that we did not apply reweighting to the LUXqed photon PDFs since the PDF uncertainty of the photon-induced cross section is already small. We see from Tables I and

II that the photon-induced cross section  $\sigma_\gamma$  and uncertainties depend on the choice of the photon PDFs. Especially, the photon PDF uncertainties decrease significantly as we change from NNPDF2.3qed and NNPDF3.0qed to MRST2004qed, CT14QEDinc, and to LUXqed. The NLO QCD corrections for various photon PDFs are of the order of +17.0% for total cross sections. The EW corrections are insensitive to the choice of the photon PDFs, and are about -7.0%. The reweighting PDF uncertainties of the photon-induced cross section  $\sigma_{\gamma PR}$  are reduced significantly after including the CMS data to reweight the NNPDF2.3qed, NNPDF3.0qed, MRS2004qed, and CT14QEDinc photon PDFs, while the corresponding central predicted cross sections are unchanged. From Table I ( $pp \rightarrow H + W^+(\rightarrow l^+\nu_l)$ ), the relative errors  $\Delta\sigma_\gamma/\sigma_\gamma$  for the photon-induced cross sections reduce from 88.7% and 89.5% in the NNPDF2.3qed and NNPDF3.0qed predictions to 5.5% and 8.2% in the reweighting NNPDF2.3qed and reweighting NNPDF3.0qed predictions; the relative errors  $\Delta\sigma_\gamma/\sigma_\gamma$  reduce from 23.9% in the MRST2004qed predictions to 7.6% in the reweighting MRST2004qed predictions; the relative errors  $\Delta\sigma_\gamma/\sigma_\gamma$  reduce from 13.4% in the CT14QEDinc predictions to 7.1% in the reweighting CT14QEDinc predictions. From Table II ( $pp \rightarrow H + W^-(\rightarrow l^-\bar{\nu}_l)$ )

PDF	NNPDF2.3qed	NNPDF3.0qed	MRST2004qed	CT14QEDinc	LUXqed
$\sigma_{LO} [fb]$	$79.06 \pm 1.15$	$78.45 \pm 1.17$	$78.75 \pm 0.03$	$78.75 \pm 0.07$	$80.59 \pm 0.13$
$\sigma_{NLO} [fb]$	$93.66 \pm 5.70$	$92.30 \pm 5.56$	$92.43 \pm 0.61$	$90.48 \pm 0.27$	$93.36 \pm 0.15$
$\sigma_\gamma [fb]$	$6.01 \pm 5.33$	$5.94 \pm 5.32$	$4.46 \pm 0.65$	$4.47 \pm 0.36$	$4.49 \pm 0.006$
$\delta_{QCD} [\%]$	$17.53 \pm 0.04$	$17.47 \pm 0.05$	$17.75 \pm 0.005$	$17.39 \pm 0.001$	$17.68 \pm 0.008$
$\delta_{EW} [\%]$	$-7.41 \pm 0.008$	$-7.43 \pm 0.009$	$-7.42 \pm 0.006$	$-7.41 \pm 0.006$	$-7.41 \pm 0.001$
$\sigma_{\gamma PR} [fb]$	$6.01 \pm 0.33$	$5.94 \pm 0.49$	$4.46 \pm 0.21$	$4.47 \pm 0.19$	$4.49 \pm 0.006$

TABLE I: The first and second rows are the total cross sections in LO and NLO; the third row is the photon-induced process cross sections; and the fourth and fifth rows are the NLO QCD and EW corrections and corresponding PDF uncertainties (68% CL) for the process  $pp \rightarrow H + W^+(\rightarrow l^+\nu_l)$  with various PDFs at the LHC at 13 TeV and Higgs boson mass  $M_H = 125$  GeV without kinematic cuts. The last row is the photon-induced process cross sections and PDF uncertainties for the various re-weighted PDFs.

we see that the relative errors  $\Delta\sigma_\gamma/\sigma_\gamma$  of the photon-induced cross sections reduce from 96.6% and 95.4% in the NNPDF2.3qed and NNPDF3.0qed predictions to 5.7% and 9.5% in the reweighting NNPDF2.3qed and reweighting NNPDF3.0qed predictions; the relative errors  $\Delta\sigma_\gamma/\sigma_\gamma$  reduce from 24.5% in the MRST2004qed predictions to 7.6% in the reweighting MRST2004qed predictions; and the relative errors  $\Delta\sigma_\gamma/\sigma_\gamma$  reduce from 11.8% in the CT14QEDinc predictions to 6.3% in the reweighting CT14QEDinc predictions. From Table III ( $pp \rightarrow H + Z(\rightarrow l^+l^-)$ ) we see that the photon-induced cross section contributions is small for various photon PDFs; the NLO QCD corrections are of the order of +17% for total cross sections; the EW corrections are insensitive to the choice of the PDF set, and are about -5%; the PDF uncertainties of the photon-induced cross sections  $\sigma_{\gamma PR}$  are reduced



PDF	NNPDF2.3qed	NNPDF3.0qed	MRST2004qed	CT14QEDinc	LUXqed
$\sigma_{LO} [fb]$	$50.41 \pm 0.73$	$49.77 \pm 0.85$	$49.35 \pm 0.02$	$49.73 \pm 0.06$	$51.36 \pm 0.09$
$\sigma_{NLO} [fb]$	$59.41 \pm 4.27$	$58.65 \pm 4.23$	$57.78 \pm 0.41$	$56.99 \pm 0.14$	$59.35 \pm 0.11$
$\sigma_{\gamma} [fb]$	$4.19 \pm 4.05$	$4.18 \pm 3.99$	$2.89 \pm 0.43$	$2.86 \pm 0.20$	$2.98 \pm 0.004$
$\delta_{QCD} [\%]$	$16.79 \pm 0.06$	$16.73 \pm 0.05$	$17.05 \pm 0.005$	$16.79 \pm 0.002$	$17.02 \pm 0.008$
$\delta_{EW} [\%]$	$-7.26 \pm 0.007$	$-7.30 \pm 0.0006$	$-7.28 \pm 0.0005$	$-7.28 \pm 0.006$	$-7.26 \pm 0.001$
$\sigma_{\gamma PR} [fb]$	$4.19 \pm 0.24$	$4.18 \pm 0.40$	$2.89 \pm 0.13$	$2.86 \pm 0.11$	$2.98 \pm 0.004$

TABLE II: The first and second rows are the total cross sections in LO and NLO; the third row is the photon-induced process cross sections; and the fourth and fifth rows are the NLO QCD and EW corrections and corresponding PDF uncertainties (68% CL) for the process  $pp \rightarrow H + W^- (\rightarrow l^- \bar{\nu}_l)$  with various PDFs at the LHC at 13 TeV and Higgs boson mass  $M_H = 125$  GeV without kinematic cuts. The last row is the photon-induced process cross sections and PDF uncertainties for the various re-weighted PDFs.

significantly after including the CMS data to reweight the various photon PDFs, while the average predicted cross sections are unchanged. For example, the relative errors  $\Delta\sigma_{\gamma}/\sigma_{\gamma}$  of the photon-induced cross sections reduce from 76.2% and 86.5% in the NNPDF2.3qed and NNPDF3.0qed predictions to 4.7% and 8.1%; in the reweighting NNPDF2.3qed and reweighting NNPDF3.0qed predictions; the relative errors  $\Delta\sigma_{\gamma}/\sigma_{\gamma}$  reduce from 17.2% in the MRST2004qed predictions to 5.1% in the reweighting MRST2004qed predictions; and the relative errors  $\Delta\sigma_{\gamma}/\sigma_{\gamma}$  reduce from 10.1% in the CT14QEDinc predictions to 3.7% in the reweighting CT14QEDinc predictions.

PDF	NNPDF2.3qed	NNPDF3.0qed	MRST2004qed	CT14QEDinc	LUXqed
$\sigma_{LO} [fb]$	$21.77 \pm 0.31$	$21.58 \pm 0.32$	$21.72 \pm 0.0006$	$21.68 \pm 0.02$	$22.26 \pm 0.03$
$\sigma_{NLO} [fb]$	$24.74 \pm 0.56$	$24.46 \pm 0.51$	$24.65 \pm 0.02$	$24.47 \pm 0.006$	$25.19 \pm 0.04$
$\sigma_{\gamma} [fb]$	$0.42 \pm 0.32$	$0.37 \pm 0.32$	$0.29 \pm 0.03$	$0.30 \pm 0.02$	$0.29 \pm 0.0003$
$\delta_{QCD} [\%]$	$16.82 \pm 0.05$	$16.71 \pm 0.05$	$17.02 \pm 0.005$	$16.79 \pm 0.002$	$17.00 \pm 0.009$
$\delta_{EW} [\%]$	$-5.14 \pm 0.005$	$-5.13 \pm 0.005$	$-5.10 \pm 0.002$	$-5.16 \pm 0.0002$	$-5.15 \pm 0.0008$
$\sigma_{\gamma PR} [fb]$	$0.42 \pm 0.02$	$0.37 \pm 0.03$	$0.29 \pm 0.006$	$0.30 \pm 0.006$	$0.29 \pm 0.0003$

TABLE III: The first and second rows are the total cross sections in LO and NLO; the third row is the photon-induced process cross sections; and the fourth and fifth rows are the NLO QCD and EW corrections and corresponding PDF uncertainties (68% CL) for the process  $pp \rightarrow H + Z (\rightarrow l^+ l^-)$  with various PDFs at the LHC at 13 TeV and Higgs boson mass  $M_H = 125$  GeV. The last row is the photon-induced process cross sections and corresponding PDF uncertainties for the various re-weighted PDFs.

## D. Fiducial Cross Section

Apart from the total cross section without any cuts, in this subsection we consider the total cross section after applying cuts to the charged leptons. In Tables IV, V, and VI we list the LO and NLO total cross sections ( $\sigma_{\text{LO}}$ ,  $\sigma_{\text{NLO}}$ ) including NLO QCD and EW corrections ( $\delta_{\text{QCD}}$ ,  $\delta_{\text{EW}}$ ), and photon-induced cross sections ( $\sigma_\gamma$ ,  $\sigma_{\gamma PR}$ ) with PDF uncertainties for the Higgs-strahlung processes  $pp \rightarrow W^\pm/Z + H \rightarrow l\nu_l/l^+l^- + H$  with kinematical cuts in Section II B with NNPDF2.3qed, NNPDF3.0qed, MRS2004qed, CT14QEDinc, and LUXqed photon PDFs and Higgs boson mass  $M_H=125$  GeV at the LHC with  $\sqrt{s}=13$  TeV. The LO and NLO total cross sections are reduced by the kinematical cuts. The NLO QCD corrections for VH do not depend on the cuts on the final state charged lepton, but the EW corrections and the photon-induced cross section do depend on them. The photon-induced cross section is only significant for WH production. It is about  $10^{-3}$  fb for the  $pp \rightarrow H + Z(\rightarrow l^+l^-)$  process, as we can see from Table VI. Note that we did not apply reweighting to the LUXqed photon PDFs, since the PDF uncertainty of the photon-induced cross section is already small. The NLO QCD corrections for various photon PDFs are of the order of +17.0% for total cross sections. The EW corrections are insensitive to the choice of the photon PDFs, and are about  $-8.0\%$  for  $W^+H$ ,  $-7.0\%$   $W^-H$  and  $-9.0\%$  for  $ZH$  with leptonic decays. We see from Tables IV and V that the photon-induced cross sections  $\sigma_\gamma$  and uncertainties depend on the choice of the photon PDFs. Especially, the photon PDF uncertainties decrease significantly as we change from NNPDF2.3qed and NNPDF3.0qed to MRST2004qed, CT14QEDinc, and to LUXqed. The reweighting PDF uncertainties of the photon-induced cross sections  $\sigma_{\gamma PR}$  are reduced significantly after including the CMS data to reweight the NNPDF2.3qed, NNPDF3.0qed, MRS2004qed, and CT14QEDinc photon PDFs, while the corresponding central predicted cross sections are unchanged. From Table IV ( $pp \rightarrow H + W^+(\rightarrow l^+\nu_l)$ ) we see that the relative errors  $\Delta\sigma_\gamma/\sigma_\gamma$  for the photon-induced cross sections reduce from 55.5% and 58.7% in the NNPDF2.3qed and NNPDF3.0qed predictions to 10.5% and 7.2% in the reweighting NNPDF2.3qed and reweighting NNPDF3.0qed predictions; the relative errors  $\Delta\sigma_\gamma/\sigma_\gamma$  reduce from 21.6% in the MRST2004qed predictions to 6.6% in the reweighting MRST2004qed predictions; the relative errors  $\Delta\sigma_\gamma/\sigma_\gamma$  reduce from 10.6% in the CT14QEDinc predictions to 5.5% in the reweighting CT14QEDinc predictions.

From Table V ( $pp \rightarrow H + W^-(\rightarrow l^-\bar{\nu}_l)$ ) we see that the relative errors  $\Delta\sigma_\gamma/\sigma_\gamma$  for the photon-induced cross section reduce from 57.6% and 62.4% in the NNPDF2.3qed and NNPDF3.0qed predictions to 10.3% and 7.4% in the reweighting NNPDF2.3qed and reweighting NNPDF3.0qed predictions; the relative errors  $\Delta\sigma_\gamma/\sigma_\gamma$  reduce from 22.2% in the MRST2004qed predictions to 6.9% in the reweighting MRST2004qed predictions; and the relative errors  $\Delta\sigma_\gamma/\sigma_\gamma$  reduce from 11.3% in the CT14QEDinc predictions to 5.9% in the reweighting CT14QEDinc predictions.

PDF	NNPDF2.3qed	NNPDF3.0qed	MRST2004qed	CT14QEDinc	LUXqed
$\sigma_{LO} [fb]$	$65.09 \pm 0.96$	$64.61 \pm 0.98$	$64.59 \pm 0.03$	$64.78 \pm 0.07$	$66.33 \pm 0.11$
$\sigma_{NLO} [fb]$	$73.64 \pm 1.80$	$72.94 \pm 1.90$	$73.58 \pm 0.29$	$72.95 \pm 0.09$	$75.05 \pm 0.12$
$\sigma_{\gamma} [fb]$	$2.56 \pm 1.42$	$2.35 \pm 1.38$	$2.40 \pm 0.32$	$2.54 \pm 0.16$	$2.51 \pm 0.003$
$\delta_{QCD} [\%]$	$17.41 \pm 0.04$	$17.41 \pm 0.04$	$17.69 \pm 0.003$	$17.36 \pm 0.02$	$17.57 \pm 0.007$
$\delta_{EW} [\%]$	$-8.27 \pm 0.01$	$-8.18 \pm 0.008$	$-8.24 \pm 0.0002$	$-8.26 \pm 0.01$	$-8.21 \pm 0.001$
$\sigma_{\gamma PR} [fb]$	$2.56 \pm 0.27$	$2.35 \pm 0.17$	$2.40 \pm 0.10$	$2.54 \pm 0.09$	$2.51 \pm 0.003$

TABLE IV: The first and second rows are the fiducial cross sections in LO and NLO; the third row is the photon-induced process fiducial cross sections; and the fourth and fifth rows are the NLO QCD and EW corrections and corresponding PDF uncertainties (68% CL) for the process  $pp \rightarrow H + W^+(\rightarrow l^+ \nu_l)$  with various PDFs at the LHC at 13 TeV and Higgs boson mass  $M_H = 125$  GeV without kinematic cuts. The last row is the photon-induced process fiducial cross sections and PDF uncertainties with various re-weighted PDFs.

PDF	NNPDF2.3qed	NNPDF3.0qed	MRST2004qed	CT14QEDinc	LUXqed
$\sigma_{LO} [fb]$	$37.70 \pm 0.52$	$37.25 \pm 0.62$	$37.23 \pm 0.18$	$37.33 \pm 0.04$	$38.46 \pm 0.07$
$\sigma_{NLO} [fb]$	$42.96 \pm 1.16$	$42.29 \pm 1.25$	$42.62 \pm 0.18$	$42.22 \pm 0.04$	$43.74 \pm 0.08$
$\sigma_{\gamma} [fb]$	$1.65 \pm 0.95$	$1.49 \pm 0.93$	$1.44 \pm 0.19$	$1.51 \pm 0.11$	$1.54 \pm 0.002$
$\delta_{QCD} [\%]$	$17.42 \pm 0.06$	$17.38 \pm 0.05$	$17.66 \pm 0.005$	$17.42 \pm 0.004$	$17.60 \pm 0.007$
$\delta_{EW} [\%]$	$-7.96 \pm 0.008$	$-7.87 \pm 0.008$	$-7.95 \pm 0.0002$	$-7.94 \pm 0.006$	$-7.89 \pm 0.001$
$\sigma_{\gamma PR} [fb]$	$1.65 \pm 0.17$	$1.49 \pm 0.11$	$1.44 \pm 0.06$	$1.51 \pm 0.05$	$1.54 \pm 0.002$

TABLE V: The first and second rows are the fiducial cross sections in LO and NLO; the third row is the photon-induced process fiducial cross sections; the fourth and fifth rows are the NLO QCD and EW corrections and corresponding PDF uncertainties (68% CL) for the process  $pp \rightarrow H + W^-(\rightarrow l^- \bar{\nu}_l)$  with various PDFs at the LHC at 13 TeV and Higgs boson mass  $M_H = 125$  GeV without kinematic cuts.

### E. Fiducial Differential Cross Section

In this subsection we consider the differential cross sections after applying cuts to the charged leptons. We plot the transverse-momentum distributions for Higgs production in  $pp \rightarrow W^\pm/Z + H \rightarrow l\nu_l/l^+l^- + H$  at LO and NLO in QCD for Higgs boson mass  $M_H = 125$  GeV with the kinematical cuts and set up described in Section II B. The  $p_T(H)$  distributions of the Higgs boson are shown in Figs. 5, 6 and 7 for various PDFs. From the NLO (upper) and LO (lower)  $p_T(H)$  distribution curves we see that the NLO correction is small at small  $p_T(H)$ , and increases slightly with  $p_T(H)$  as the cross section falls rapidly. The upper left plot is the transverse-momentum distributions of Higgs boson production at LO (lower curves) and NLO (upper curves) including NLO QCD and EW corrections. The lower left plot is the photon correction  $\delta_\gamma = d\sigma_\gamma/d\sigma_{LO}$  and EW corrections  $\delta_{EW}$  for various PDFs. The EW

PDF	NNPDF2.3qed	NNPDF3.0qed	MRST2004qed	CT14QEDinc	LUXqed
$\sigma_{LO} [fb]$	$13.50 \pm 0.18$	$13.64 \pm 0.20$	$13.48 \pm 0.006$	$13.44 \pm 0.01$	$14.05 \pm 0.02$
$\sigma_{NLO} [fb]$	$14.63 \pm 0.20$	$14.76 \pm 0.22$	$14.65 \pm 0.006$	$14.58 \pm 0.02$	$15.24 \pm 0.02$
$\sigma_\gamma [fb]$	$1 \times 10^{-3}$	$6 \times 10^{-3}$	$2 \times 10^{-3}$	$2 \times 10^{-3}$	$7 \times 10^{-3}$
$\delta_{QCD} [\%]$	$17.37 \pm 0.05$	$17.30 \pm 0.04$	$17.67 \pm 0.003$	$17.45 \pm 0.003$	$17.53 \pm 0.009$
$\delta_{EW} [\%]$	$-9.01 \pm 0.008$	$-9.15 \pm 0.008$	$-9.01 \pm 0.0002$	$-8.99 \pm 0.004$	$-9.15 \pm 0.001$

TABLE VI: The first and second rows are the fiducial cross sections in LO and NLO; the third row is the photon-induced process fiducial cross sections; and the fourth and fifth rows are the NLO QCD and EW corrections and corresponding PDF uncertainties (68% CL) for the process  $p p \rightarrow H + Z(\rightarrow l^+ l^-)$  with various PDFs at the LHC at 13 TeV and Higgs boson mass  $M_H = 125$  GeV.

correction for the process  $pp \rightarrow H + W(\rightarrow l\nu_l)$  grows further negative to (10–20)% as  $p_T(H)$  increases. The photon-induced corrections have a tendency to grow as well, but can reach only 2.5% level. In the top right plot we show transverse-momentum distributions of various PDF predictions to LUXqed prediction. The bottom right panel is the ratio of  $\delta_\gamma/\delta_{\gamma LUXqed}$ .

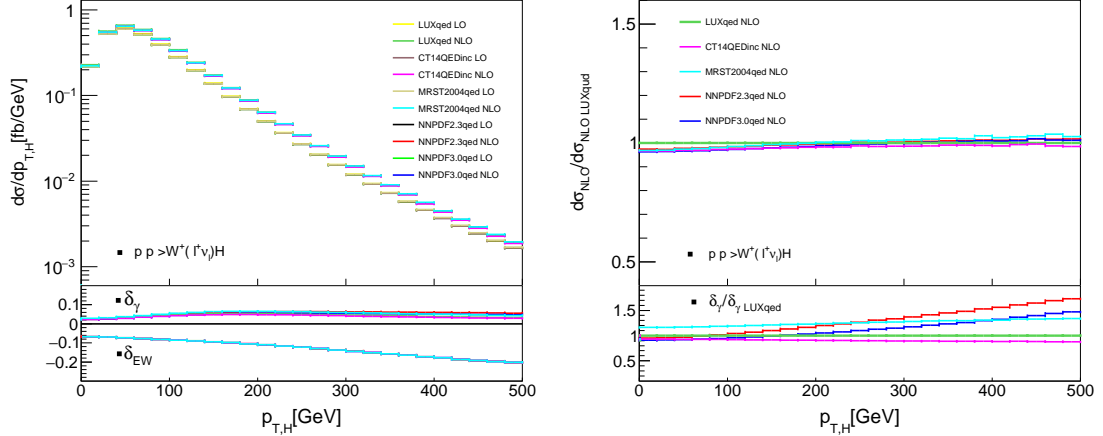


FIG. 5: Fiducial differential cross section distributions (top left panel) both at LO (lower curves) and NLO (upper curves) and ratio of  $d\sigma_{NLO}/d\sigma_{NLO LUXqed}$  (top right panel) of the Higgs boson in  $W^+(l^+\nu_l)H$  production after applying the selection cuts in Section IIB at the LHC at 13 TeV for the various PDFs. The bottom left panel shows the electroweak  $\delta_{EW}$  and photon corrections  $\delta_\gamma = d\sigma_\gamma/d\sigma_{LO}$ . The bottom right panel is the ratio of  $\delta_\gamma/\delta_{\gamma LUXqed}$ .

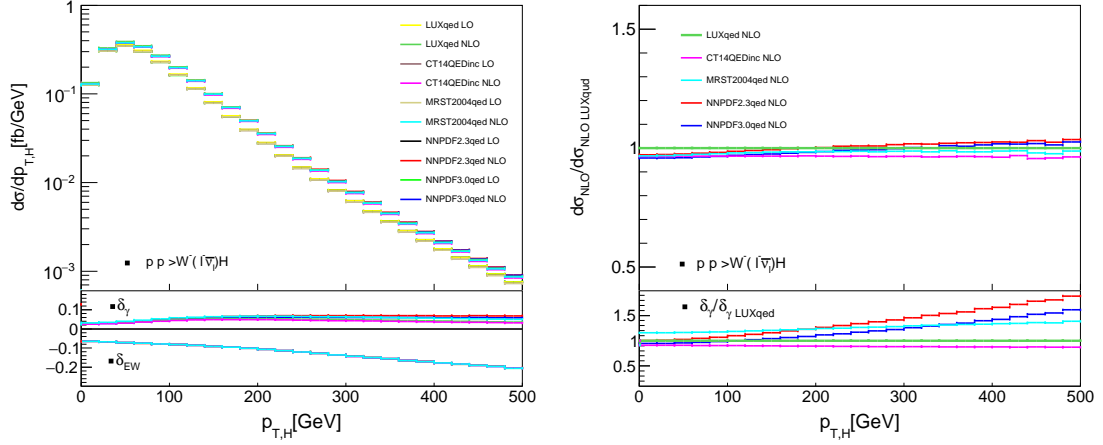


FIG. 6: Differential cross section distributions (top left panel) both at LO (lower curves) and NLO (upper curves) and ratio of  $d\sigma_{NLO}/d\sigma_{NLO LUXqed}$  (top right panel) of the Higgs boson in  $W^-(l^-\bar{\nu}_l)H$  production after applying the selection cuts in section II B at the LHC at 13 TeV for the various PDFs. The bottom left panel shows the electroweak  $\delta_{EW}$  and photon corrections  $\delta_\gamma = d\sigma_\gamma/d\sigma_{LO}$ . The bottom right panel is the ratio of  $\delta_\gamma/\delta_\gamma LUXqed$ .

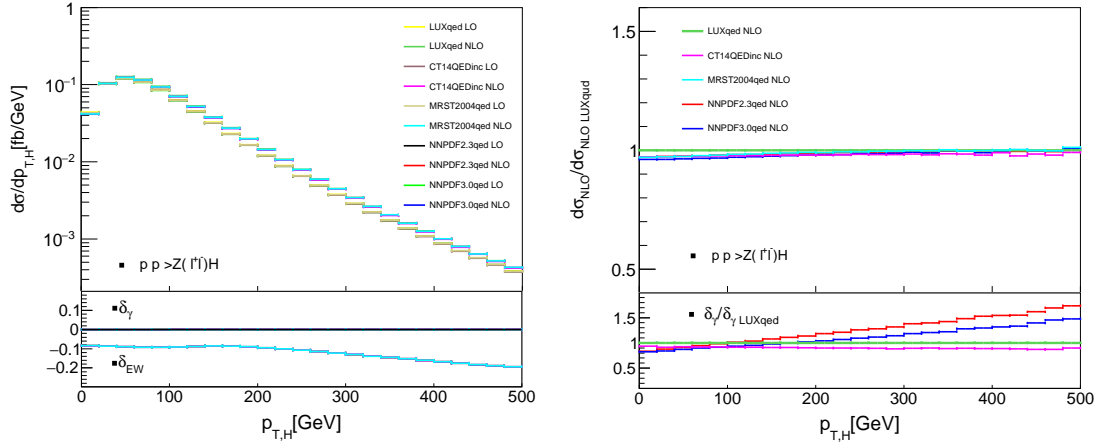


FIG. 7: Differential cross section distributions (top left panel) both at LO (lower curves) and NLO (upper curves) and ratio of  $d\sigma_{NLO}/d\sigma_{NLO LUXqed}$  (top right panel) of the Higgs boson in  $Z(l^+l^-)H$  production after applying the selection cuts in section II B at the LHC at 13 TeV for the various PDFs. The bottom left panel shows the electroweak  $\delta_{EW}$  and photon corrections  $\delta_\gamma = d\sigma_\gamma/d\sigma_{LO}$ . The bottom right panel is the ratio of  $\delta_\gamma/\delta_\gamma LUXqed$ .

### III. CONCLUSIONS

We have calculated the NLO QCD and EW corrections to Higgs boson production in association with  $W$  and  $Z$  bosons at the LHC at 13 TeV and with Higgs boson mass  $M_H = 125$  GeV for various PDFs using the HAWK Monte Carlo tool within the  $G_\mu$ -scheme. The total cross sections and fiducial cross sections for the processes  $pp \rightarrow W^\pm + H \rightarrow l\nu_l + H$  and  $pp \rightarrow Z + H \rightarrow l^+l^- + H$  were given in Tables I, II, III, IV, V, and VI. The EW corrections to  $W^+(\rightarrow l^+\nu_l)H$ ,  $W^-(\rightarrow l^-\bar{\nu}_l)H$  and  $Z(\rightarrow l^+l^-)H$  productions decrease the total cross sections by about -7.4%, -7.3% and -5.1% respectively. The NLO QCD corrections to  $W^+(\rightarrow l^+\nu_l)H$ ,  $W^-(\rightarrow l^-\bar{\nu}_l)H$  and  $Z(\rightarrow l^+l^-)H$  productions increase the total cross sections by about 17.5%, 17.0% and 17.0% respectively. Our photon-induced process fiducial cross sections in Tables IV, V, and VI agree well with the results of Ref. [9] in their Tables 5.7, 5.8, and 5.9; and our EW corrections in Tables I - III, and IV - VI agree well with the results of Ref. [9] in their Tables 5.3-5.5 and 5.7-5.9. The PDF uncertainties of the photon-induced process cross sections are reduced significantly for NNPDF2.3qed, NNPDF3.0qed, MRS2004qed, and CT14QEDinc photon PDF sets after including the CMS 8 TeV data. Especially, the CMS data can have a very large impact in reducing the NNPDF photon PDF errors.

### IV. ACKNOWLEDGMENTS

We thank Carl Schmidt and C.-P. Yuan for many very helpful discussions. This work is supported by the National Natural Science Foundation of China under the Grant No. 11465018.

- 
- [1] For a review of the Higgs sector, see : J.F. Gunion, H.E. Haber, G.L. Kane and S. Dawson, The Higgs Hunter's Guide, Addison-Wesley, Reading 1990.
  - [2] T. Han, S. Willenbrock, FERMILAB-PUB-91/70-T, BNL-45990(1991)
  - [3] M.L. Ciccolini, S. Dittmaier, M. Krämer, arXiv:hep-ph/0306234
  - [4] J. Pumplin, D. R. Stump, J. Huston, *et al.*, JHEP, 0207:012(2002) arXiv:hep-ph/0201195
  - [5] O. BREIN , A. DJOUADI, R. HARLANDER, arXiv:hep-ph/0307206
  - [6] O. Brein, M. Ciccolini, S. Dittmaier, *et al.*, arXiv: hep-ph/0402003
  - [7] A.D. Martin, R.G. Roberts, W.J. Stirling *et al.*, Phys. Lett. B, 531:216-224(2002)
  - [8] A. Denner, S. Dittmaier, S. Kallweit, *et al.*, arXiv:1112.5142
  - [9] The Working Group for standard model Higgs-Boson Searches, LHCHXSWG-DRAFT-INT-2016-008.
  - [10] A. D. Martin et al., Eur. Phys. J. C, 63:189(2009) arXiv:0901.0002
  - [11] A. D. Martin, R. G. Roberts, W. J. Stirling, *et al.*, Eur. Phys. J. C, 39:155(2005) arXiv:hep-ph/0411040.

- [12] R. D. Ball *et al.* (NNPDF Collaboration), Nucl. Phys. B, 877:4370(2013) arXiv:1308.0598
- [13] Mamut Ababekri, Sayipjamal Dulat, Joshua Isaacson *et al.*, arXiv: 1603.04874
- [14] R. D. Ball *et al.* (NNPDF Collaboration), JHEP, **1504**:040 (2015) arXiv:1410.8849
- [15] C. Schmidt, J. Pumplin, D. Stump *et al.*, arXiv:1509.02905
- [16] A. Manohar, P. Nason, G. P. Salam *et al.*, arXiv:1607.04266
- [17] <http://omnibus.uni-freiburg.de/sd565/programs/hawk/hawk.html>, 2010.
- [18] W. T. Giele and S. Keller, Phys. Rev. D, **58**:094023 (1998) arXiv:hep-ph/9803393
- [19] R. D. Ball *et al.* (NNPDF Collaboration), Nucl. Phys. B, **849**:112 (2011) Erratum: [Nucl. Phys. B, **854**:926 (2012)] Erratum: [Nucl. Phys. B, **855**:927 (2012)] arXiv:1012.0836
- [20] R. D. Ball *et al.*, Nucl. Phys. B, **855**:608 (2012) arXiv:1108.1758
- [21] N. Sato, J. F. Owens and H. Prosper, Phys. Rev. D, **89**, no. 11:114020 (2014)
- [22] V. Khachatryan *et al.* (CMS Collaboration), arXiv:1604.04464